Optica Applicata, Vol. XLIV, No. 4, 2014
DOI: 10.5277/oa140413

Photonic band gap in negative ternary refractive indices of two-dimensional photonic crystal

ABDOLRASOUL GHARAATI*, LEILA MOHAMADEBRAHIMI, ZAHRA ROOZITALAB

Department of Physics, Payame Noor University, Iran

*Corresponding author: agharaati@pnu.ac.ir

In this paper, we study propagation of electromagnetic wave in negative ternary refractive indices of two-dimensional photonic crystals. We consider two structures with two concentric cylindrical rod and shell in which one of them has negative refractive indices, in positive dielectric background. It is shown that by increasing the diameter of the rod in both structures, we can obtain more and wider band gaps in comparison with the structures in which there is no negative refractive index materials. This increase is more considerable in the first structure, in which the rod has a negative refractive index, in comparison with the second one, where the rod has a positive refractive index.

Keywords: negative refraction, two dimensional photonic crystals, metamaterials, band gaps.

1. Introduction

In the past decade, there have been much research activities relating to photonic crystals (PCs). They have attracted great attentions of researchers for their rich physics and potential applications. PCs are periodic dielectric structures with refractive indices periodicity of the order of the light wavelength. They can prohibit propagation of electromagnetic waves within a certain frequency range, so the light can be totally reflected. Such forbidden band is called photonic band gaps (PBGs) which is similar to the electronic band gaps for electrons in semiconductors [1–8].

In 2000, SMITH and co-workers [9] demonstrated in their work that it is possible to fabricate an artificial metamaterial with electrodynamics characteristics that can be described by a negative index of refraction n. The metamaterials can be divided into two categories. The first one is double-negative metamaterials whose permittivity ε and permeability μ are simultaneously negative. These metamaterials cannot be easily found in nature, but they are artificially fabricated. The other category is single-negative metamaterials which can be also divided into two categories. In the first configuration, the permittivity is positive but the permeability is negative. It is so-called μ-negative materials. In the second, the permittivity is negative but the permeability is positive. They are called ε-negative materials [10, 11]. These materials can be found easily in

nature, such as plasma, superconductor, semiconductor and metal. This kind of PCs can be used to design the omnidirectional reflector [12], multiple-channelled filter [13], tunable filter [14] and so on. In double-negative metamaterials, the direction of Poynting vector $\mathbf{S} = \mathbf{E} \times \mathbf{H}$, is opposite to the wave vector **k**, so the wave vector and a refractive index should be negative then, **k**, **E** and **H** form a left-handed set of vectors [6, 15]. The refractive index in these medium is $n = -\sqrt{\varepsilon\mu}$. The behaviors of these materials are the same as positive refraction index material.

There are many published works on the properties of one-dimensional (1D) [16, 17], two-dimensional (2D) [18–20], and recently, many works have been done on three-dimensional (3D) [21–24] PCs structure, which is more applicable in comparison with the 1D or 2D case. Here, we focus on 2D PCs which are periodic in x and y directions and homogeneous along z direction.

In this paper, by applying the boundary conditions in Maxwell equations in periodic structures, we change them to Helmholtz equation. By solving it in 2D and using a plane wave expansion method (PWEM), we can find the band gaps and allowed transfer electric (TE) and transfer magnetic (TM) modes. We consider two structures with two concentric cylindrical rod and shell; in the first structure, the rod and shell have negative and positive refractive index material, respectively and the background has positive dielectric. But, in the second structure, we change the material of the rod and shell inversely and the background is the same as the first structure. Finally, for validity of our work, we have drawn the density of state (DOS) diagram which is another important factor for the many unusual optical properties of the PCs. The DOS is the number of the eigen-states inside the unit frequency range. It provides much more information in comparison with the PBG maps because it has information about the PC behavior outside the PBGs while the PBG maps give only the knowledge about the PBGs. Low or zero DOS corresponds to the absence of the eigen-states within the corresponding frequency range, that is, the PBG. If a single state is introduced into the PBG, then the DOS of the system is zero in the PBG [25].

2. Theoretical model

In this section, we investigate the propagation of electromagnetic waves in a 2D PC with a negative refractive index. We consider two structures. The first one is composed of a concentric cylindrical rod and shell in which the radius of the rod is R_1 ($R_2 > R_1$) and its dielectric permittivity is ε_n and the radius of the shell is R_2 with dielectric permittivity ε_{d_1} in a positive refractive index background ε_{d_2}, Fig. 1**a**. In the second one, the rod and shell are inverse, but the background is the same as the first structure, Fig. 1**b**.

Here, we consider band gaps of 2D PC based on Helmholtz equation in which they are calculated by using well-known software based on PWE method. We change the cylinder radius. Then, we study the band gaps. According to this point, the simulated results of the band structure for TM and TE modes of 2D PC are demonstrated. The plane wave expansion method leads to the following equations [8, 26]:

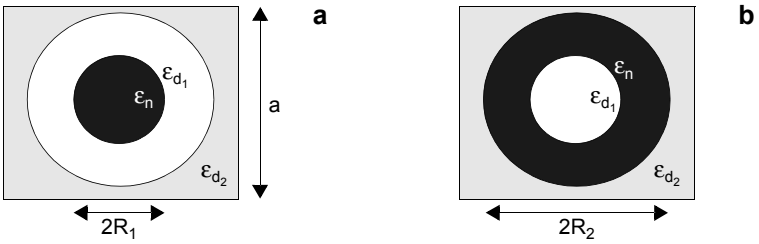

Fig. 1. Schematic structures of concentric rod and shell with radius R_1 and R_2 ($R_2 > R_1$), **a** – in the first structure, the rod filled with a negative refractive index ε_n, and the shell with a positive refractive index ε_{d_1}, and **b** – in the second structure, the rod filled with a positive refractive index ε_{d_1}, and the shell with a negative refractive index ε_n, and the background dielectric permittivity of both structures is ε_{d_2}.

$$\text{TM:} \quad \sum_{G'} \kappa(G-G')\left|k_t+G'\right|^2 E_{z,k_t}(G') = \omega_{k_t}^2 E_{z,k_t}(G)$$

$$\text{TE:} \quad \sum_{G'} \kappa(G-G')(k_t+G')(k_t+G) H_{z,k_t}(G') = \omega_{k_t}^2 H_{z,k_t}(G)$$

where $E_{z,k_t}(G)$ and $H_{z,k_t}(G)$ are the Fourier coefficients of the electric and magnetic field, respectively; k is the 2D wave vector, t denotes transverse component of a vector confined to the plane of PC and $\kappa(G-G') = \kappa_\varepsilon(G-G')\kappa_\mu(G-G')$ where

$$\kappa_\varepsilon(G-G') \equiv \begin{cases} \left(\frac{1}{\varepsilon_n}-\frac{1}{\varepsilon_{d_1}}\right)f_1+\left(\frac{1}{\varepsilon_{d_1}}-\frac{1}{\varepsilon_{d_2}}\right)f_2+\frac{1}{\varepsilon_{d_2}} & \text{if} \quad G=G' \\ \left(\frac{1}{\varepsilon_n}-\frac{1}{\varepsilon_{d_1}}\right)2f_1C_1+\left(\frac{1}{\varepsilon_{d_1}}-\frac{1}{\varepsilon_{d_2}}\right)2f_2C_2 & \text{if} \quad G\neq G' \end{cases}$$

$$\kappa_\mu(G-G') \equiv \begin{cases} \left(\frac{1}{\mu_n}-\frac{1}{\mu_{d_1}}\right)f_1+\left(\frac{1}{\mu_{d_1}}-\frac{1}{\mu_{d_2}}\right)f_2+\frac{1}{\mu_{d_2}} & \text{if} \quad G=G' \\ \left(\frac{1}{\mu_n}-\frac{1}{\mu_{d_1}}\right)2f_1C_1+\left(\frac{1}{\mu_{d_1}}-\frac{1}{\mu_{d_2}}\right)2f_2C_2 & \text{if} \quad G\neq G' \end{cases}$$

$$C_1 = \frac{J_1((G-G')R_1)}{(G-G')R_1}$$

$$C_2 = \frac{J_1((G-G')R_2)}{(G-G')R_2}$$

So, we have

$$\kappa(G-G') \equiv \begin{cases} A_1 f_1^2 + A_2 f_2^2 + A_3 f_1 + A_4 f_2 + A_5 f_1 f_2 - A_6 & \text{if} \quad G = G' \\ 4A_1 f_1^2 C_1^2 + 4A_2 f_2^2 C_2^2 + 4A_7 f_1 f_2 C_1 C_2 & \text{if} \quad G \neq G' \end{cases}$$

where

$$A_1 = \frac{1}{\varepsilon_n \mu_n} - \frac{1}{\varepsilon_n \mu_{d_1}} - \frac{1}{\varepsilon_{d_1} \mu_n} + \frac{1}{\varepsilon_{d_1} \mu_{d_1}}$$

$$A_2 = \frac{1}{\varepsilon_{d_1} \mu_{d_1}} - \frac{1}{\varepsilon_{d_1} \mu_{d_2}} - \frac{1}{\varepsilon_{d_2} \mu_{d_1}} + \frac{1}{\varepsilon_{d_2} \mu_{d_2}}$$

For the second structure we have:

$$\kappa_\varepsilon(G-G') \equiv \begin{cases} \left(\frac{1}{\varepsilon_{d_1}} - \frac{1}{\varepsilon_n}\right) f_1 + \left(\frac{1}{\varepsilon_n} - \frac{1}{\varepsilon_{d_2}}\right) f_2 + \frac{1}{\varepsilon_{d_2}} & \text{if} \quad G = G' \\ 2\left(\frac{1}{\varepsilon_{d_1}} - \frac{1}{\varepsilon_n}\right) f_1 C_1 + 2\left(\frac{1}{\varepsilon_n} - \frac{1}{\varepsilon_{d_2}}\right) f_2 C_2 & \text{if} \quad G \neq G' \end{cases}$$

$$\kappa_\mu(G-G') \equiv \begin{cases} \left(\frac{1}{\mu_{d_1}} - \frac{1}{\mu_n}\right) f_1 + \left(\frac{1}{\mu_n} - \frac{1}{\mu_{d_2}}\right) f_2 + \frac{1}{\mu_{d_2}} & \text{if} \quad G = G' \\ 2\left(\frac{1}{\mu_{d_1}} - \frac{1}{\mu_n}\right) f_1 C_1 + 2\left(\frac{1}{\mu_n} - \frac{1}{\mu_{d_2}}\right) f_2 C_2 & \text{if} \quad G \neq G' \end{cases}$$

$$\kappa(G-G') \equiv \begin{cases} B_1 f_1^2 + B_2 f_2^2 + B_3 f_1 + B_4 f_2 + B_5 f_1 f_2 + B_6 & \text{if} \quad G = G' \\ 4B_1 f_1^2 C_1^2 + 4B_2 f_2^2 C_2^2 + 4B_5 f_1 f_2 C_1 C_2 & \text{if} \quad G \neq G' \end{cases}$$

where:

$$A_1 = \frac{1}{\varepsilon_n \mu_n} - \frac{1}{\varepsilon_n \mu_{d_1}} - \frac{1}{\varepsilon_{d_1} \mu_n} + \frac{1}{\varepsilon_{d_1} \mu_{d_1}}$$

$$A_2 = \frac{1}{\varepsilon_{d_1} \mu_{d_1}} - \frac{1}{\varepsilon_{d_1} \mu_{d_2}} - \frac{1}{\varepsilon_{d_2} \mu_{d_1}} + \frac{1}{\varepsilon_{d_2} \mu_{d_2}}$$

$$A_3 = \frac{1}{\varepsilon_{d_1}\mu_{d_2}} - \frac{1}{\varepsilon_n \mu_{d_2}} + \frac{1}{\varepsilon_{d_2}\mu_n} - \frac{1}{\varepsilon_{d_2}\mu_{d_1}}$$

$$A_4 = \frac{1}{\varepsilon_{d_2}\mu_{d_1}} - \frac{1}{\varepsilon_{d_1}\mu_{d_2}}$$

$$A_5 = \frac{1}{\varepsilon_n \mu_{d_1}} - \frac{1}{\varepsilon_n \mu_{d_2}} - \frac{2}{\varepsilon_{d_1}\mu_{d_1}} + \frac{1}{\varepsilon_{d_1}\mu_{d_2}} + \frac{1}{\varepsilon_{d_2}\mu_{d_1}} - \frac{1}{\varepsilon_{d_2}\mu_n} + \frac{1}{\varepsilon_{d_1}\mu_n}$$

$$A_6 = B_6 = \frac{1}{\varepsilon_{d_2}\mu_{d_2}}$$

$$A_7 = -\frac{1}{\varepsilon_n \mu_{d_2}} - \frac{1}{\varepsilon_{d_2}\mu_n} - \frac{2}{\varepsilon_{d_1}\mu_{d_1}} + \frac{1}{\varepsilon_{d_1}\mu_{d_2}} + \frac{1}{\varepsilon_{d_2}\mu_{d_1}} + \frac{1}{\varepsilon_n \mu_{d_1}} + \frac{1}{\varepsilon_{d_1}\mu_n}$$

$$B_1 = \frac{1}{\varepsilon_{d_1}\mu_{d_1}} - \frac{1}{\varepsilon_{d_1}\mu_n} - \frac{1}{\varepsilon_n \mu_{d_1}} + \frac{1}{\varepsilon_n \mu_n}$$

$$B_2 = \frac{1}{\varepsilon_n \mu_n} - \frac{1}{\varepsilon_n \mu_{d_2}} - \frac{1}{\varepsilon_{d_2}\mu_n} + \frac{1}{\varepsilon_{d_2}\mu_{d_2}}$$

$$B_3 = \frac{1}{\varepsilon_{d_2}\mu_{d_1}} - \frac{1}{\varepsilon_n \mu_{d_2}} - \frac{1}{\varepsilon_{d_2}\mu_n} + \frac{1}{\varepsilon_{d_1}\mu_{d_2}}$$

$$B_4 = \frac{1}{\varepsilon_n \mu_{d_2}} - \frac{2}{\varepsilon_{d_2}\mu_{d_2}} + \frac{1}{\varepsilon_{d_2}\mu_n}$$

$$B_5 = -\frac{2}{\varepsilon_n \mu_n} + \frac{1}{\varepsilon_n \mu_{d_2}} - \frac{1}{\varepsilon_{d_2}\mu_{d_1}} + \frac{1}{\varepsilon_{d_2}\mu_n} + \frac{1}{\varepsilon_n \mu_{d_1}} - \frac{1}{\varepsilon_{d_1}\mu_{d_2}} + \frac{1}{\varepsilon_{d_1}\mu_n}$$

$$C_1 = \frac{J_1((G-G')R_1)}{(G-G')R_1}$$

$$C_2 = \frac{J_1((G-G')R_2)}{(G-G')R_2}$$

and the radius of the rod, shell and the lattice constant are R_1, R_2 and a, respectively. Also, f_1 and f_2 are given by $f_1 = \pi R_1^2/a^2$ and $f_2 = \pi R_2^2/a^2$; $J_1(G-G')$ is the Bessel function; ε_n, ε_{d_1}, ε_{d_2} and μ_n, μ_{d_1}, μ_{d_2} are the dielectric permittivity and permeability of the rod (shell), shell (rod) and background of the first (second) structure, respectively.

In order to compute the DOS, it is not enough to compute the PC eigen-sates at several points of the Brillouin zone, because the information obtained in such a way is not complete. The computation of the DOS consists in counting the number of eigen--states having the specific frequency which can be expressed by

$$N(\omega) = \sum_n \int_{BZ} \mathrm{d}^2 k \, \delta(\omega - \omega_n(K))$$

where the multiplication by the δ-function extracts the eigen-states with the same frequency. Then, the integration is carried out. This means summation of eigen-states with the same frequencies within one band. After integration, the summation over all the bands is carried out.

3. Results and discussion

In this section, we investigate the band gaps, the DOS and gap map diagrams of both structures for TM and TE modes. First, we draw the band structures and the DOS diagrams for the first structure. Let us $\varepsilon_n = -1.94$, $\varepsilon_{d_1} = 12$, $\varepsilon_{d_2} = 8.9$, $\mu_n = -1$ and $\mu_{d_1} = \mu_{d_2} = 1$, $R_2 = 0.5a$ and we change R_1 from $0.1a$ to $0.4a$ by step 0.1. By increasing the radius of the rod which is made of negative refractive index material, we obtain more and wider gaps, as it has been shown in Figs. 2–5. In Figure 2, we take $R_1 = 0.2a$ and $R_2 = 0.5a$. Drawing the band structure and DOS diagram for TM mode shows that we have a wide gap in comparison with the structure with a positive refractive index. In Figure 3, on the other hand, we take $R_2 = 0.5a$ and increase the radius of rod to $R_1 = 0.4a$. We see that the number of band gaps increase with respect to the previous state.

Now, we investigate the band structures and DOS diagrams for TE mode. Again, we consider $R_2 = 0.5a$ and change R_1 from $0.1a$ to $0.4a$ by step 0.1. In Figure 4, we

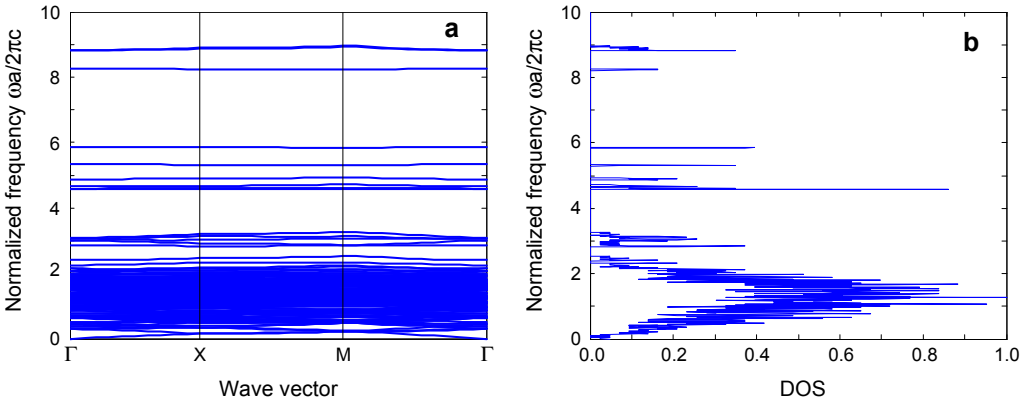

Fig. 2. The band structure (**a**) and DOS diagram (**b**) of the first structure for TM mode, $\varepsilon_n = -1.94$, $\varepsilon_{d_1} = 12$, $\varepsilon_{d_2} = 8.9$, $R_1 = 0.2a$ and $R_2 = 0.5a$.

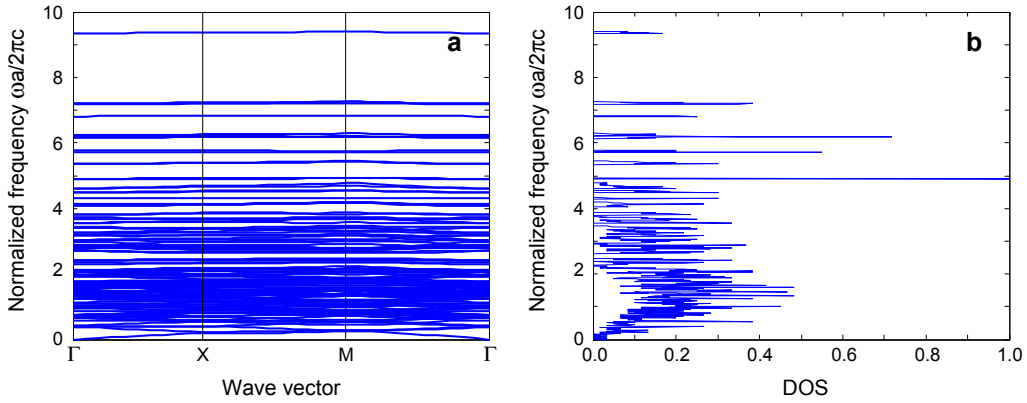

Fig. 3. The same as Fig. 2 but $R_1 = 0.4a$.

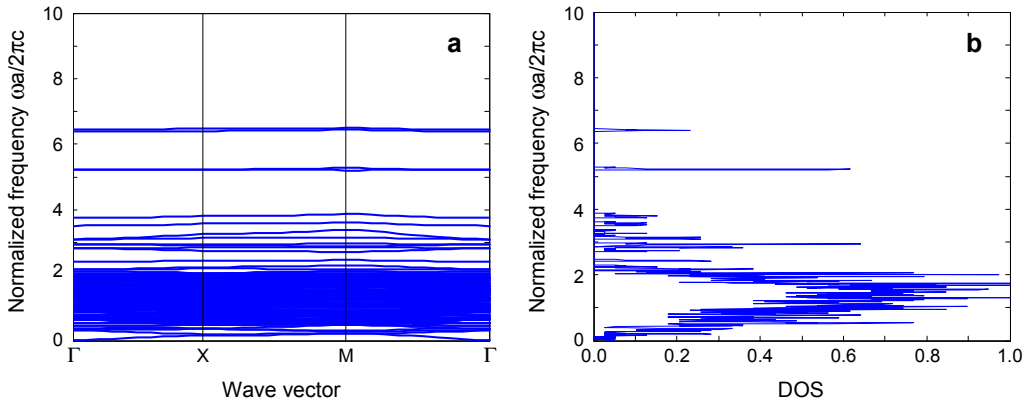

Fig. 4. The same as Fig. 2, but for TE mode.

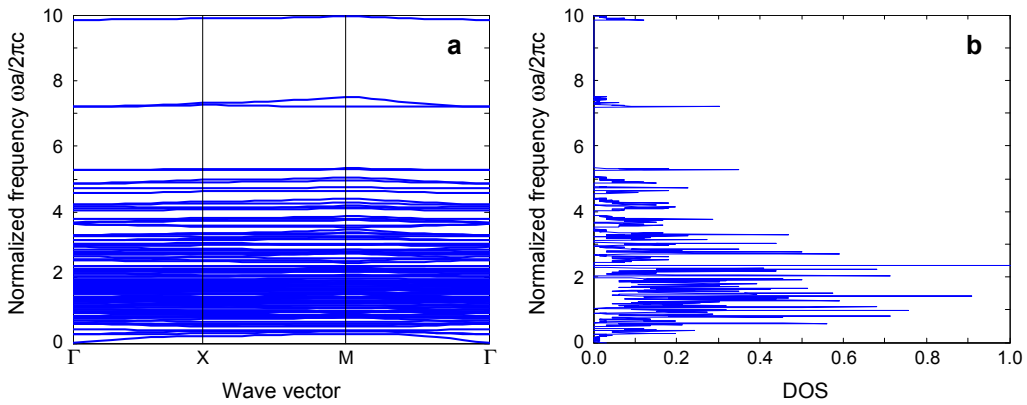

Fig. 5. The same as Fig. 4, but $R_1 = 0.4a$.

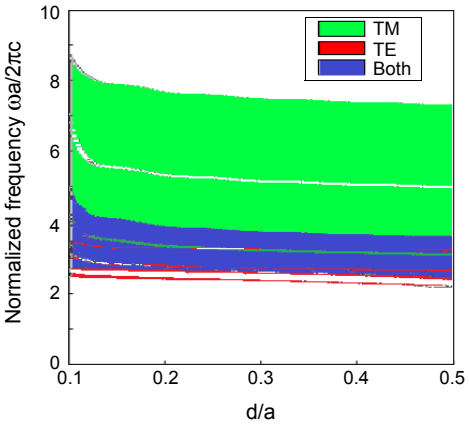

Fig. 6. Gap map diagram of the first structure. The green and red areas show TM and TE modes and the blue one shows the common area (omnidirectional reflectors).

increase the radius of rod to $R_1 = 0.2a$ and we obtain a lot of wider gaps. In Figure 5 we increase R_1 from $0.2a$ to $0.4a$. We obtain more and wider gaps with respect to Fig. 4.

Then, we draw the gap map diagram of the first structure for both TM and TE modes. We see that the area of TM mode is more than the TE one in this diagram. A common area has been seen in both modes, Fig. 6. In this figure, the green and red areas show TM and TE modes and the blue one shows the common area (omnidirectional reflectors) of these modes.

On the other hand, we plot the band structure and DOS diagram of TM mode for the second structure. We see that by increasing the radius of the rod which is made of positive refractive index material up to $R_1 = 0.2a$ (Fig. 7), $R_1 = 0.4a$ (Fig. 8), we obtain more and wider gaps in comparison with the structure with a positive refractive index, but it is not as considerable as the first structure. In this figure, d/a is the ratio of di-

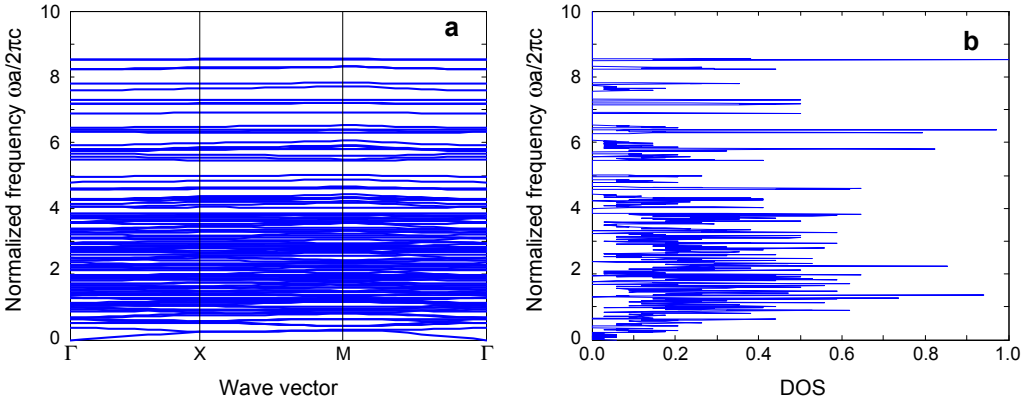

Fig. 7. The same as Fig. 2, but for the second structure.

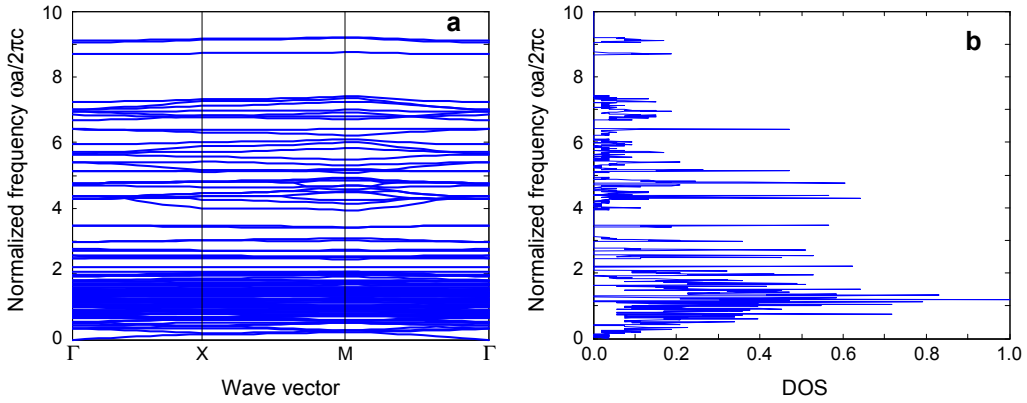

Fig. 8. The same as Fig. 7, but $R_1 = 0.4a$.

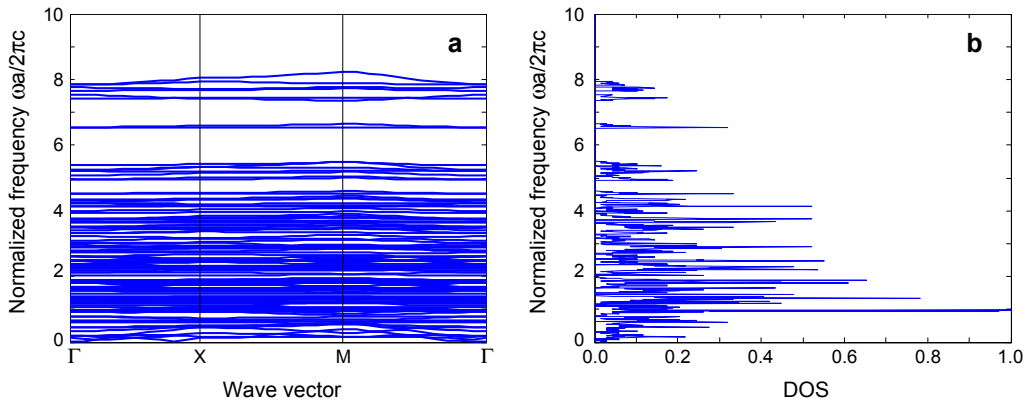

Fig. 9. The same as Fig. 7, but for TE mode.

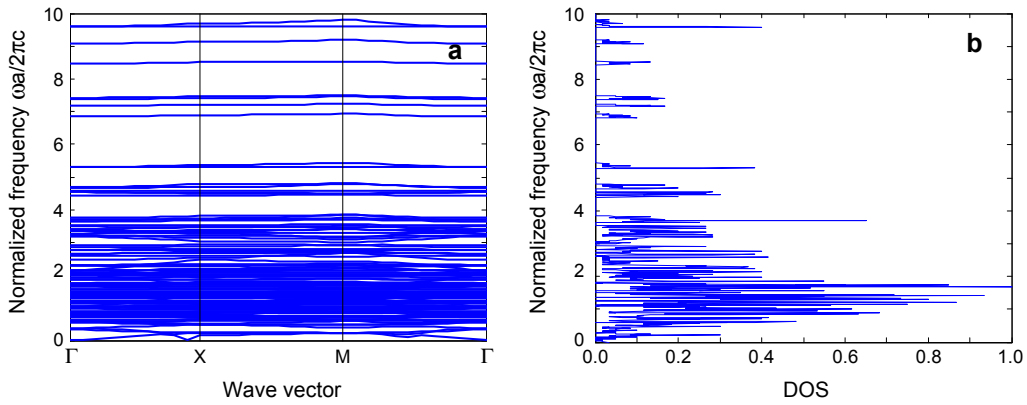

Fig. 10. The same as Fig. 9, but $R_1 = 0.4a$.

ameter to constant lattice and d is the diameter of a clad on cylinder with radius of R_1 (*i.e.*, $d = R_2 - R_1$).

Finally, we investigate the band structures of TE mode for the second structure. Again, we consider $R_2 = 0.5a$ and we change R_1 from $0.1a$ to $0.4a$ by step 0.1. By increasing the radius of the rod up to $R_1 = 0.2a$ (Fig. 9), we have several wide gaps. When we increase the radius rod to $R_1 = 0.4a$ (Fig. 10), we see that the number and width of gaps are more considerable than the previous state.

Then, we draw the gap map diagram of the second structure for both TM and TE modes. A common area can be seen in both modes, Fig. 11.

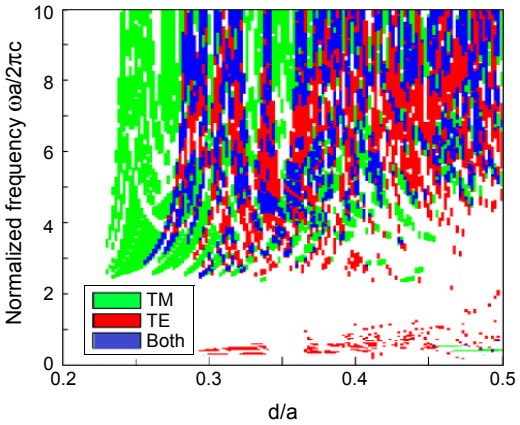

Fig. 11. Gap map diagram of the second structure. The green and red areas show TM and TE modes and the blue one shows the common area (omnidirectional reflectors).

We have observed that when $R_1 = 0$ and $R_2 = 0.5a$ ($R_1 = 0.5a$ and $R_2 = 0.5a$) in the first structure, the band structures are completely the same as the second one in the case $R_1 = 0.5a$ and $R_2 = 0.5a$ ($R_1 = 0$ and $R_2 = 0.5a$). In these cases, they have unique structures. The colourful areas in this figure are the same as in Fig. 6.

4. Conclusions

In this paper, we have drawn the band structures, the DOS and gap map diagrams of negative ternary refractive indices in 2D PCs including rod, shell and background for two structures. It has been observed that by increasing the radius of the rod in both structures, we have obtained more and wider band gaps for both TM and TE modes in comparison with the structures with all positive refractive index material. It is just because of the existence of negative refractive index material in these structures. The increase in number and width of gaps, is more considerable in the first structure. Drawing the gap map diagrams of both structures shows that we have wider gaps in the first

structure in comparison with the second one. If we replace positive refractive index materials instead of the negative one, we will not have any band gaps in any radius of both structures.

Acknowledgments – This work has been financially supported by the Payame Noor University (PNU).

References

[1] SALEH B.E.A., TEICH M.C., *Fundamental of Photonics*, 2nd Ed., Wiley, New York 2007.
[2] SUKHOIVANOV A., GURYEV V., *Photonic Crystals Physics and Practical Modelling*, Springer Series in Optical Science, New York, 2009.
[3] JOANNOPOULOS J.D., MEADE R.D., WINN J.N., *Photonic Crystals, Molding the Flow of Light*, 2nd Ed., Princeton University Press, Princeton, 1995.
[4] MARUDUDIN A.A., MCGURN A.R., *Photonic band structure of a truncated, two-dimensional periodic dielectric medium*, Journal of the Optical Society of America B **10**(2), 1993, pp. 307–313.
[5] MEADE R.D., RAPPE A.M., BROMMER K.D., JOANNOPOULOS J.D., *Nature of the photonic band gap: some insights from a field analysis*, Journal of the Optical Society of America B **10**(2), 1993, pp. 328–332.
[6] RAMAKRISHNA S.A., *Physics of negative refractive index materials*, Reports on Progress in Physics **68**(2), 2005, pp. 449–521.
[7] MARKOS P., SOUKOULIS C.M., *Wave Propagation: From Electrons to Photonic Crystals and Left-Handed Materials*, Princeton University Press, Canada, 2008.
[8] SKOROBOGATIY M., YANG J., *Fundamentals of Photonic Crystal Guiding*, 1st Ed., Cambridge University Press, 2009.
[9] SMITH D.R., PADILLA W J., VIER D.C., NEMAT-NASSER S.C., SCHULTZ S., *Composite medium with simultaneously negative permeability and permittivity*, Physical Review Letters **84**(18), 2000, pp. 4184–4187.
[10] VESELAGO V.G., *The electrodynamics of substance with simultaneously negative values of ε and μ*, Soviet Physics Uspekhi **10**(4), 1968, pp. 509–514.
[11] MARQUÉS R., MARTÍN F., SOROLLA M., *Metamaterials with Negative Parameters: Theory, Design and Microwave Applications*, Wiley Series in Microwave and Optical Engineering, 2007.
[12] XIN-HUA DENG, JIANG-TAO LIU, JIE-HUI HUANG, LINER ZOU, NIAN-HUA LIU, *Omnidirectional bandgaps in Fibonacci quasicrystals containing single-negative materials*, Journal of Physics: Condensed Matter **22**(5), 2010, article 055403.
[13] XU JING-PING, HE LI, QIAO WEN-TAO, ZHANG LI-WEI, *Electromagnetic tunnelling properties of sandwich structure containing single negative material*, Acta Physica Sinica **59**(11), 2010, pp. 7863–7868.
[14] LIU SHAO-BIN, ZHANG HAI-FENG, KONG XIANG, *Analsys of the properties of tunable prohibited band gaps for two-dimensional unmagnetized plasma photonic crystals under TM mode*, Acta Physica Sinica **60**(5), 2011, article 055209.
[15] ENGHETA N., ZIOLKOWSKI R.W., *Metamaterials Physics and Engineering Exploration*, John Wiley and Sons, USA, 2006.
[16] GHARAATI A., ZARE Z., *Photonic band structures and enhancement of omnidirectional reflection bands by using a ternary 1D photonic crystal including left-handed materials*, Progress in Electromagnetics Research M **20**, 2011, pp. 81–94.
[17] ZARE Z., GHARAATI A., *Investigation of band gap width in ternary 1D photonic crystal with left--handed layer*, Acta Physica Polonica A **125**(1), 2014, pp. 36–38.
[18] VESELAGO V., BRAGINSKY L., SHKLOVER V., HAFNER C., *Negative refractive index materials*, Journal of Computational and Theoretical Nanoscience **3**(2), 2006, pp. 189–218.

[19] CHIYAN LUO, JOHNSON S.G., JOANNOPOULOS J.D., PENDRY J.B., *All-angle negative refraction without negative effective index*, Physical Review B **65**, 2002, article 201104(R).

[20] ZIOLKOWSKI R.W., HEYMAN E., *Wave propagation in media having negative permittivity and permeability*, Physical Review E **64**, 2001, article 056625.

[21] HAI-FENG ZHANG, SHAO-BIN LIU, XIANG-KUN KONG, *Investigation of the unusual surface plasmon modes and switching band gap in three-dimensional photonic crystals with pyrochlore lattices composed of epsilon-negative materials*, Journal of the Optical Society of America B **31**(6), 2014, pp. A31–A39.

[22] HAI-FENG ZHANG, SHAO-BIN LIU, *The anisotropic photonic band gaps in three-dimensional photonic crystals with high-symmetry lattices composed of metamaterials and uniaxial materials*, Optical Materials, **36**(5), 2014, pp. 903–910.

[23] ZHANG H.-F., LIU S.-B., LI H.-M., *The wavelength division multiplexer realized in three-dimensional unusual surface-plasmon-induced photonic crystals composed of the epsilon-negative materials shells*, Progress in Electromagnetics Research **144**, 2014, pp. 151–169.

[24] HAI-FENG ZHANG, SHAO-BIN LIU, XIANG-KUN KONG, *Investigating the dispersive properties of the three-dimensional photonic crystals with face-centered-cubic lattices containing epsilon-negative materials*, Applied Physics B **112**(4), 2013, pp. 553–563.

[25] LOURTIOZ J.-M., BENISTY H., BERGER V., GERARD J.-M., MAYSTRE D., TCHELNOKOV A., *Photonic Crystals – Towards Nanoscale Photonic Devices*, Springer, Heidelberg, 2005.

[26] BELL P.M., PENDRY J.B., MORENO L.M., WARD A.J., *A program for calculating photonic band structures and transmission coefficients of complex structures*, Computer Physics Communications **85**(2), 1995, pp. 306–322.

Received May 14, 2014
in revised form July 18, 2014